

**Antimicrobial applications of electroactive PVK-SWNT nanocomposites**

Journal:	<i>Environmental Science &amp; Technology</i>
Manuscript ID:	Draft
Manuscript Type:	Article
Date Submitted by the Author:	n/a
Complete List of Authors:	Ahmed, Farid; University of Houston, Civil and Environmental Engineering Santos, Catherine; University of Houston, Civil and Environmental Engineering Vergara, Regina; University of Houston, Department of Chemistry Tria, Maria Celeste; University of Houston, Department of Chemistry and Chemical Engineering Advincula, Rigoberto; University of Houston, Chemistry Rodrigues, Debora; University of Houston, Civil and Environmental Engineering

SCHOLARONE™  
Manuscripts

# Antimicrobial applications of electroactive PVK-SWNT nanocomposites

*Farid Ahmed,<sup>a</sup> Catherine M. Santos,<sup>a</sup> Regina Aileen May V. Vergara,<sup>b,c</sup> Maria Celeste R. Tria,<sup>b</sup>  
Rigoberto Advincula,<sup>b,c</sup> and Debora F. Rodrigues<sup>a\*</sup>*

<sup>a</sup> Department of Civil and Department of Environmental Engineering  
University of Houston, Houston, TX 77204-5003 (USA)

<sup>b</sup> Department of Chemistry and Department of Chemical and Biomolecular Engineering  
University of Houston, Houston, TX 77240-5003 USA

<sup>c</sup> Graduate School University of Santo Tomas, Manila, Philippines

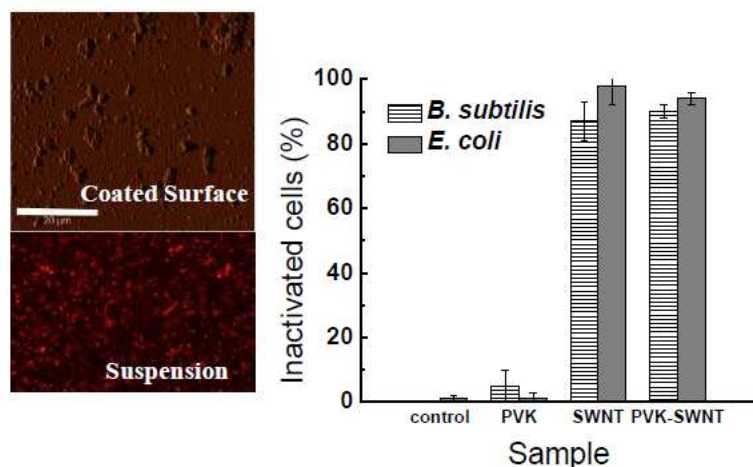
E-mail: dfrigirodrigues@ uh.edu

**RECEIVED DATE (to be automatically inserted after your manuscript is accepted if required  
according to the journal that you are submitting your paper to)**

Corresponding Author: E-mail: dfrigirodrigues@ uh.edu; Tel: 713-743-1495; Fax: 713-743-4260

## ABSTRACT

## Antimicrobial PVK-SWNT Nanocomposite



The antibacterial properties of a nanocomposite containing an electroactive polymer, polyvinyl-*N*-carbazole (PVK), (97 wt %) and single-walled carbon nanotubes (SWNT) (3 wt %) was investigated as suspensions in water and thin film coatings. The toxic effects of four different PVK-SWNT (97:3 wt%) nanocomposite concentrations (1, 0.5, 0.05 and 0.01 mg/ml) containing 0.03, 0.015, 0.0015, and 0.0003 mg/ml of SWNT, respectively, were determined for planktonic cells and biofilms of *Escherichia coli* (*E. coli*) and *Bacillus subtilis* (*B. subtilis*). The results showed that the nanocomposite PVK-SWNT had antibacterial activity on planktonic cells and biofilms at all concentration levels. Higher bacterial inactivation (94% for *E. coli* and 90% for *B. subtilis*) were achieved in planktonic cells at a PVK-SWNT concentration of 1mg/ml. Atomic force microscopy (AFM) imaging showed significant reduction of biofilm growth on PVK-SWNT coated surfaces. This study established for the first time that the improved dispersion of SWNTs in aqueous solutions in the presence of PVK enhances the antimicrobial effects of SWNTs at very low concentrations. Furthermore, PVK-SWNT can be used as an effective thin film coating material to resist biofilm formation.

KEYWORDS : SWNT, PVK, antibacterial, nanocomposite, coating

## Introduction

Materials used in aquatic environments and medical devices have high potential for biofilm formation.<sup>1</sup> Biofilms are complex aggregations of microorganisms surrounded by an extracellular matrix and have been reported to grow on conducting and exposed surfaces of biomedical devices, marine and industrial instruments, and pipes. Biofilm growth has led to several health and economic problems. The problems include antibiotic-resistant infections, increased energy consumption, excessive operational expenditures, and accelerated corrosion problems.<sup>2</sup> To solve these problems, different types of coatings, that can protect the surface from biofilm formation, have been developed, such as polyamide and polypropylene with silver<sup>3, 4</sup>, antibiotics<sup>4-7</sup>, quaternary ammonium salts,<sup>8</sup> cationic peptides,<sup>9</sup> and metal ions<sup>10</sup>. However the syntheses of biofilm resistant surfaces tend to be complex and expensive, and often the surfaces loose effectiveness due to leaching or depletion of the antimicrobial agents.<sup>5-7</sup>

Recently, several studies have shown that single-walled-carbon nanotubes (SWNTs) have antimicrobial properties against diverse groups of microorganisms like bacteria (both Gram-positive and Gram-negative), protozoa, and viruses.<sup>8-12</sup> SWNT-coated surfaces has also been shown to significantly inhibit *E. coli* biofilm formation.<sup>7</sup> However, the use of SWNT as antimicrobial agent is still limited by its poor dispersibility in most solvents as well as its high cost.<sup>5, 13, 14</sup> Alternatively, SWNT combined (as a filler component) with polymers provide better dispersion and can potentially increase or maintain the same antimicrobial properties of SWNT materials, while providing a broad range of structural, mechanical, and degradation properties.<sup>1, 5, 15</sup> Unfortunately, there have only been a handful of studies about antibacterial effects of polymer-SWNT nanocomposites. None of them have explored the possibility of using these composites as robust coating materials to resist biofilm formation. Electroactive polymers are an excellent choice for such nanocomposites, because of its anti-corrosion properties and facile surface application (via electrodeposition).<sup>16, 17</sup> Among the available electroactive polymers, polyvinyl-*N*-carbazole (PVK) is an excellent candidate due to its good thermal and mechanical properties, and its ability to form robust thin films (i.e. conducting polymer network (CPN)) on any conducting surface.<sup>18, 19</sup> Furthermore, PVK contains the aromatic *N*-carbazole group that facilitate  $\pi$ - $\pi$  stacking as well as

donor-acceptor interactions making it a more compatible polymer for carbon-based nanomaterials like SWNT.<sup>20, 21</sup>

In this study, we investigated the PVK-SWNT nanocomposite antibacterial properties to planktonic cells (i.e. cells in suspension prior to biofilm formation) and biofilms. The bacterial toxicity of different concentrations of PVK-SWNT dispersed in water were investigated against Gram-positive (*B. subtilis*) and Gram-negative (*E. coli*) bacteria, as well as the potential inhibition properties of biofilm formation on coated surfaces with the PVK-SWNT nanocomposite. The results showed for the first time that by improving dispersibility of SWNT in solution, higher bacterial toxicity of SWNT can be achieved, even in concentrations as low as 0.0003 mg/mL of SWNT. Furthermore, PVK-SWNT coated surfaces with only 3% of SWNTs significantly inhibited biofilm formation. This result shows that coated surfaces for antimicrobial purposes can be made with reduced concentrations of SWNT.

## Materials and Methods

*Single-walled carbon nanotubes (SWNT) preparation:* Single-walled carbon nanotubes (SWNTs) were purchased from Cheap Tubes Inc. (Vermont, US). The characterization of these nanomaterials can be found in the Supporting Information (SI) section (Table S1, Table S2 and Figure S1). The SWNTs were further purified by heating at 200 °C for 6 hours prior to use.

*PVK-SWNT nanocomposite solutions:* The poly (N-vinyl carbazole) (PVK) was purchased from Sigma-Aldrich Chemicals (USA) (ca MW= 25,000-50,000 g/mol). All solvents used for the PVK-SWNT preparation were purchased from Sigma Aldrich (USA) and were of analytical grade. The PVK-SWNT (97:3 wt% ratio PVK: SWNT) was prepared according to previously reported procedure.<sup>16</sup> The PVK:SWNT ratio of 97:3 (wt%) was selected based on the high dispersibility and stability of SWNT for long periods of time (several months) as described in our previous work.<sup>22</sup> Briefly, a 97:3 wt/vol % ratio of PVK:SWNT was prepared in *N*-cyclohexyl-2-pyrrolidone (CHP). The purified SWNT was first dissolved in CHP and sonicated for 4 h. Then, in a separate vial, the PVK was dissolved in CHP and sonicated for 30 min. The PVK solution was then slowly mixed to the SWNT solution and followed by

sonication for 1 h. After which, the PVK-SWNT dispersion was centrifuged (4400 rpm, 1 h) and the black precipitate was removed. The remaining solution of PVK-SWNT dispersion was then treated with methanol (5 mL) and again centrifuged (4400 rpm) for 30 min. The black precipitate was collected and redispersed in water followed by 20 minutes of ultrasonication. This procedure furnished a stable and well dispersed PVK-SWNTs solution. For the bacterial measurements, different PVK-SWNT concentrations (1.0 mg/ml, 0.5 mg/ml, 0.05 mg/ml, and 0.01 mg/ml) dispersions in water were used. The SWNT concentrations (mg/ml) from the prepared PVK-SWNT (97:3 wt %) dispersions are provided in Table 1.

**Table 1.** SWNT concentration on the PVK-SWNT (97:3 wt %) dispersed in aqueous solution

PVK-SWNT (97:3 wt%) concentration (mg/ml)	Representative SWNT concentration (mg/ml)
1.00	0.03
0.50	0.015
0.05	0.0015
0.01	0.0003

*Preparation of PVK-SWNT nanocomposite CPN films:* Indium tin oxide (ITO)-coated glass slides (Alfa Aeser, USA) were used as substrates for the PVK-SWNT, PVK, SWNT film fabrication. The ITO-coated glass slides were cleaned by sequentially sonicating the slides in deionized (dI) water, isopropanol, hexane and toluene, each for 15 minutes and the substrates were dried under a stream of N<sub>2</sub>. Prior to film deposition, the ITO surfaces were plasma cleaned for 3 min. The electropolymerization solution was prepared by mixing 0.1 M tetrabutylammonium hydroxide (TBAH) (2 mL) in acetonitrile with PVK (50 µL) or PVK-SWNT suspension (50 µL) at 97:3 (wt %) ratio as described above. The PVK-SWNT and PVK films were deposited onto bare ITO surfaces by repeatedly scanning the potential between 0 and 1500 mV at a scan rate of 10 mV/s for 50 cycles. Ag and Pt wires were used as reference and counter electrode, respectively, for the electrodeposition of PVK-SWNT. The deposited film was

1 rinsed three times with acetonitrile to remove any unbound material from the surface.  
2  
3  
4

5  
6 *Characterization of PVK-SWNT nanocomposite:* The PVK-SWNT dispersions were characterized by  
7  
8 Fourier transformed infrared spectroscopy (FTIR) and UV-vis absorption measurements. FTIR images  
9  
10 were obtained using -FTS 7000 Digilab Spectrometer in the range of 700-3500  $\text{cm}^{-1}$ . UV-vis spectra of  
11  
12 the PVK-SWNT dispersion and electrodeposited film were recorded using an Agilent 8453  
13  
14 spectrometer.  
15  
16

17  
18 The electrodeposition of PVK-SWNT conducting polymer network (CPN) films onto ITO were  
19  
20 monitored by acquiring the cyclic voltammogram plots (Princeton Applied Research Parsat 2263) at  
21  
22 each cycle. The nanocomposite (PVK-SWNT) crosslinked films were characterized using X-ray  
23  
24 photoelectron spectroscopy and UV-vis measurements. XPS measurements of the samples were  
25  
26 performed using a PHI 5700 X-ray photoelectron spectrometer (XPS), which was equipped with a  
27  
28 monochromatic Al  $K\alpha$  X-ray source ( $h\nu = 1486.7 \text{ eV}$ ) incident at  $90^\circ$  relative to the axis of a  
29  
30 hemispherical energy analyzer. The spectrometer was operated both at high and low resolutions with  
31  
32 pass energies of 23.5 and 187.85 eV, respectively, a photoelectron take off angle of  $45^\circ$  from the  
33  
34 surface, and an analyzer spot diameter of 1.1 mm. High-resolution spectra were obtained for  
35  
36 photoelectrons emitted from C 1s and N 1s. All spectra were collected at room temperature with a base  
37  
38 pressure of  $1 \times 10^{-8}$  torr. Electron binding energies were calibrated with respect to the C1s line at 284.8  
39  
40 eV. PHI Multipak software (ver 5.0A) was used for all data processing. The high-resolution data was  
41  
42 first analyzed by background subtraction using the Shirley routine and a subsequent nonlinear fitting to  
43  
44 mixed Gaussian-Lorentzian functions. Atomic compositions were derived from the high-resolution  
45  
46 scans. Peak areas were obtained after subtraction of the integrated baseline and corrected for sensitivity  
47  
48 factors.  
49  
50  
51  
52  
53  
54  
55  
56  
57  
58  
59  
60

*Bacterial Culture and Antimicrobial Activity determined by OD measurements:* Single isolated colonies of *E. coli* MG 1655 and *B. subtilis* 102 were inoculated and incubated in 5 ml of Tryptic Soya Broth (TSB) (Oxoid, England) overnight at 35 °C and 200 rpm. The bacterial culture was centrifuged at 3000 rpm for 10 minutes. The cells were washed and re-suspended in phosphate buffer solution (PBS, 0.01M, pH=7.4) (Fisher Scientific, USA). The bacterial suspension was adjusted to give an optical density (OD) of 0.5 at 600 nm, which corresponds to a concentration of 10<sup>7</sup> colony forming units (CFU)/ml. For the antimicrobial activity assay, bacterial cultures were exposed for 1 h to the different nanomaterials. Briefly, aliquots of 180 µl of bacterial suspensions (10<sup>7</sup> CFU/ml) in PBS and non-inoculated PBS buffer with bacteria (used as blanks) were pipeted in a 96-well flat bottom plate (Costar 3370, Corning, NY) containing triplicates of 20 µl of the following samples suspended in DI water: (1) SWNT at concentration of 1.0 mg/ml; (2) PVK-SWNT nanocomposite at concentrations of 1.0 mg/ml, 0.5 mg/ml, 0.05 mg/ml, and 0.01 mg/ml; and (3) 1 mg/ml of PVK. The control samples contained 20 µl of DI water only with 180µl of bacterial suspensions. To account for the absorbance of SWNT and PVK-SWNT nanomaterials suspended in the bacterial samples, 20 µl of each concentration of SWNT and PVK-SWNT were added to 180 µl of PBS only and later used as blanks to subtract from the original samples. The plates were then incubated at 37°C at 50 rpm for 1h. After 1 h, 20 µl of the bacteria exposed to the different materials, the negative controls, and the blank samples were transferred into 96 well-plates containing 200 µl TSB. The samples were then incubated at 37 °C at 50 rpm and the bacterial growth was monitored using Synergy MX Microtiter plate reader (BioTek, VT) by measuring the OD<sub>600</sub> every hour until the bacteria reached stationary phase. The results for *E. coli* and *B. subtilis* growth after exposure to the nanomaterials were reported at their mid-log phases, i.e. after 3 h and 5 h, respectively (SI, Figure S4). Final OD values for each bacterial solution exposed to the different nanomaterial samples were determined by subtracting the OD values acquired from their respective blanks. The results are reported as average OD values with standard deviations of the triplicate samples from all three performed experiments. Statistical analyses (Two-sided t-Test, 95% confidence interval) were performed to determine whether the OD values of the samples with SWNT or PVK-SWNT were



1 significantly different from the control. Same statistical analysis was also performed between OD values  
2  
3 from SWNT and PVK-SWNT samples.  
4  
5  
6

7 *Plate agar test:* The plate agar test was performed on modified ITO substrates as previously described.<sup>23</sup>  
8  
9 The unmodified ITO, electrodeposited PVK-SWNT (97:3 wt %), electrodeposited PVK, and spin coated  
10 SWNT-modified films on ITO were individually placed in a 12 well-plate (Falcon, USA). To each well  
11  
12 was added 1.0 ml of bacterial culture, which was incubated at 37 °C (without shaking) for 2 h. As a  
13  
14 control for potential contamination during manipulation of the ITO substrates, unmodified surfaces  
15  
16 incubated in PBS were also used. The film samples were removed and gently rinsed with PBS to wash  
17  
18 any unattached bacteria to the surface. The surfaces were then placed onto a Tryptic Soy Agar (TSA)  
19  
20 plate with the coated side facing down onto the agar surface and incubated overnight at 35 °C. The  
21  
22 bacterial growth around each plate was measured using a caliper micrometer Mitutoyo 500-196-20  
23  
24 Digital Caliper (MSI Viking Gage, USA). Averages and standard deviations were calculated from 3  
25  
26 replicates.  
27  
28  
29  
30  
31  
32  
33  
34  
35

36 *Live/Dead Assay:* Live/Dead assay was performed using the LIVE/DEAD BacLight kit (Invitrogen,  
37  
38 USA) to quantify the number of live and dead cells after interaction of the bacterial cells with the most  
39  
40 toxic concentrations of nanomaterial samples determined by “*the OD measurement assays of*  
41  
42 *antimicrobial activity*”. The assay consisted of mixing 20 µl of the most toxic concentrations of  
43  
44 nanomaterials for each bacteria with 180 µl of bacterial suspensions at 0.5 OD and incubated for one  
45  
46 hour at 35 °C. After 1 hr incubation, 10 µl of the suspension was stained with the LIVE/DEAD BacLight  
47  
48 Bacterial Viability kit and observed under Fluorescence Microscope (OLYMPUS, Japan). SYTO 9 dye  
49  
50 was used to stain live cells and propidium iodide (PI) was used to stain cells with compromised  
51  
52 membranes.<sup>24</sup> Three representative images at 40x were taken for each sample and all samples were  
53  
54 tested in duplicate. Total cells and dead cells were counted with Image-Pro Plus software  
55  
56 (MediaCybernetics, USA). The percent of inactivated cells was determined from the ratio of the number  
57  
58  
59  
60

1 of cells stained with PI divided by the number of cells stained with SYTO-9 plus PI. The results were  
2 averaged out and the standard deviations were calculated.  
3  
4  
5  
6

7 *Biofilm formation assay with OD measurement:* In this assay, we measured the total biofilm growth  
8 under exposure of different concentrations of nanomaterials as previously described.<sup>7</sup> Biofilm growth  
9 was measured by using 96-well flat bottom plate (Costar 3370, Corning, NY). The concentrations of  
10 nanomaterials used in this assay were (1) SWNT at concentration of 1.0 mg/ml; (2) PVK-SWNT  
11 nanocomposite at concentrations of 1.0 mg/ml, 0.5 mg/ml, 0.05 mg/ml, and 0.01 mg/ml; and (3) 1  
12 mg/ml of PVK. The control samples contained only DI water instead of nanomaterials. The 96-well  
13 plate was prepared with bacteria and nanocomposites following the same procedure as described in  
14 “Antimicrobial Activity determined by OD measurements” section. For both *E. coli* and *B. subtilis*,  
15 plates were prepared in triplicate. After inoculation of bacteria with the nanomaterials, the 96-well plates  
16 were incubated at 35 °C for 48 hr and then stained according to crystal violet staining method for  
17 biofilm quantification described elsewhere.<sup>23</sup> Briefly, supernatant from the wells in the plate were  
18 poured out and the plate was washed three times. For staining, 300 µl of 0.1% crystal violet was added  
19 in each well and incubated for 20 minutes in room temperature. After incubation, the staining solution  
20 was poured out and washed three times. In each well 300 µl of ethanol solution in acetone (80 %  
21 vol/vol) was added and the plate was read at OD<sub>540</sub>. The results are expressed as average OD values with  
22 standard deviations using all triplicates. Statistical analyses were performed as described in the  
23 “Bacterial Culture and Antimicrobial Activity determined by OD measurements” section.  
24  
25  
26  
27  
28  
29  
30  
31  
32  
33  
34  
35  
36  
37  
38  
39  
40  
41  
42  
43  
44  
45  
46

47 *Biofilm formation measurements on nanocomposite coated surface:* Inhibition of biofilm growth were  
48 determined on nanocomposite coated ITO surfaces. Unmodified ITO, electrodeposited PVK-SWNT  
49 (97:3 wt % PVK: SWNT), electrodeposited PVK, and spin coated SWNT-modified films on ITO were  
50 individually placed in a 12-well plate (FalconBD, USA). Each well of the 12-well plate, containing  
51 TSB, were inoculated with 300 µl of bacterial cells at OD of 0.5 and incubated at 37 °C for 48 hr. After  
52  
53  
54  
55  
56  
57  
58  
59  
60

1 incubation, the ITO surfaces were taken out and gently rinsed with sterile DI water. Biofilm fixation was  
2 done according to cell fixation method previously described.<sup>25</sup> Briefly, the ITO surfaces were incubated  
3 with 2% glutaraldehyde and subsequently dehydrated with increasing concentrations of ethanol (25%,  
4 50%, 75%, 95% and 100%). The surfaces were vacuum dried overnight prior to AFM measurements.  
5  
6  
7  
8  
9  
10 AFM topography measurements were done on the ITO substrates under ambient conditions with a  
11 PicoSPM II (PicoPlus, Molecular Imaging-Agilent Technologies) in the intermittent contact mode.  
12  
13  
14 Images obtained were processed using Gwyddion software (2.13).  
15  
16  
17  
18  
19

## 20 Results and Discussion:

21  
22 *PVK-SWNT characterization:* The dispersion of PVK-SWNT (97-3 wt %) nanocomposites were  
23 characterized using FT-IR and UV-vis. FT-IR measurements confirmed the functional groups present on  
24 the nanocomposite (Figure S2). As controls, IR measurements of PVK and SWNT were also acquired.  
25  
26  
27 As expected, no distinctive IR peaks were observed for the pure SWNT. However, the PVK-SWNT  
28  
29  
30  
31  
32 nanocomposite showed similar peaks to pure PVK. In particular, the peak at  $1255\text{ cm}^{-1}$ , due to the C-N  
33  
34 stretching of vinyl carbazole, was observed in both PVK and PVK-SWNT nanocomposite.  
35  
36

37 UV-vis spectra of the PVK-SWNT dispersion were acquired to measure interfacial interaction of  
38 SWNT and PVK. Results are shown in Figure S2(b). Based on the results, no absorption peaks at the  
39 visible region were observed for pure SWNT. The pure PVK however showed two distinct peaks at 330  
40 and 343 nm, which can be attributed to the transitions of the pendant carbazole moieties of PVK.<sup>26</sup>  
41  
42  
43  
44  
45  
46 Similar absorption peaks were observed for the PVK-SWNT nanocomposite with a slight decrease in  
47  
48  
49 intensity and red-shifted by ~10 nm due to the incorporation of SWNT.  
50

51 Electrodeposited PVK-SWNT coated surfaces were characterized using XPS to determine  
52 elemental composition on the surface. Figure S3 (a) and S3 (b) shows the narrow scans in the N1s and  
53  
54  
55  
56  
57  
58  
59  
60 C1s of the electrodeposited PVK-SWNT and PVK surfaces. To estimate the amount of SWNT after  
electrocrosslinking, N/C ratios of PVK-SWNT and PVK were acquired. For PVK-SWNT, a calculated

1 N/C ratio value of 9.4 was obtained while for PVK, the N/C ratio was calculated as 9.7. Using the  
2 obtained N/C ratios, the amount of PVK and SWNT on the film was 97 % and 3 %, respectively.  
3

4  
5 UV-Vis spectra after electrodeposition of the PVK-SWNT, Figure S3(c), showed the  
6 disappearance of the well-defined peaks at 342 nm and 352 nm that were initially found for the PVK-  
7 SWNT dispersion (Figure S2 b). A new broad band centered at 450 nm was depicted after the  
8 electrodeposition process, attributed to the electrochemical crosslinking of the carbazole pendants in  
9 PVK.<sup>27, 28</sup> These results correlates well with our previous studies on electropolymerized PVK and  
10 carbazole-containing precursors.<sup>26, 28</sup>  
11  
12  
13  
14  
15  
16  
17  
18  
19  
20

21 *Antibacterial effects of nanocomposites in planktonic cells:* The toxic effects of PVK-SWNT, PVK, and  
22 SWNT solutions to *E. coli* and *B. subtilis* were evaluated by OD<sub>600</sub> measurements of the total bacterial  
23 growth. The OD values for *E. coli* cells exposed to SWNT and PVK-SWNT samples were ~27% and  
24 ~29% lower than the control samples, respectively. Similarly, the OD values for *B. subtilis* cells exposed  
25 to SWNT and PVK-SWNT were ~ 5% and ~20% lower than the controls, respectively (Figure 1). These  
26 results demonstrated that the effects of SWNT and PVK-SWNT to *E. coli* and *B. subtilis* were not the  
27 same; however these findings were similar to other studies.<sup>5, 29, 30</sup> The different levels of tolerance of  
28 different microorganisms to carbon-based nanomaterials are still a matter of continuing research. Several  
29 hypotheses for the different toxicity levels consider differences in cell wall structure, the protective  
30 effect of the outer membrane surface properties, ability to form spores and/or unique repair mechanisms  
31 of different microorganisms.<sup>31</sup> It is noticeable that PVK itself did not exhibit any antibacterial effects on  
32 either *E. coli* or *B. subtilis* (Figure 1). Furthermore, the results show that after 1 hr of exposure to SWNT  
33 and PVK-SWNT nanocomposite fewer bacteria were viable. This was demonstrated by the much longer  
34 time for the remaining microbial population to reach mid-log phase than the control samples.<sup>32, 33</sup>  
35  
36  
37  
38  
39  
40  
41  
42  
43  
44  
45  
46  
47  
48  
49  
50  
51  
52  
53  
54  
55  
56  
57  
58  
59  
60

it was necessary at least 5 mg/ml of SWNT to achieve similar toxic levels to our study. These higher toxic levels of PVK-SWNTs with SWNTs in lower concentrations than pure SWNT can be explained by a better dispersion of the SWNTs in aqueous solution in the presence of PVK as previously demonstrated.<sup>16</sup> This better dispersion of the SWNTs particles in aqueous media is because of the effective pi-pi stacking and donor-acceptor interactions between the carbazole group and the SWNT. In the case of SWNT toxicity towards bacteria, dispersion is an important parameter and highly dispersed SWNT causes greater cell contact and can potentially increase cell damage.<sup>9, 13</sup> Hence, it may be hypothesized that despite a much less SWNT content (0.003mg/ml) in the PVK-SWNT nanocomposite, the higher toxic effects of this nanocomposite compared to the pure SWNTs is possibly due to a better dispersion of the PVK-SWNT in the solution, which increases the effective contact area of SWNT with the microorganisms.

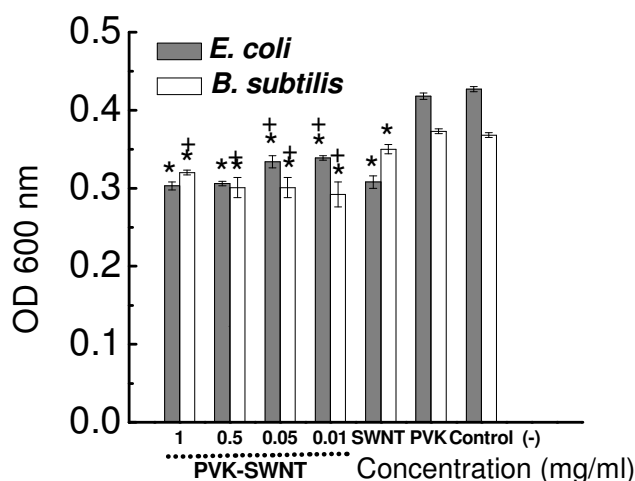


**Figure 1.** OD measurements of the bacterial growth at mid-log phase for *E. coli* and *B. subtilis* after 1 h exposure to nanomaterials. Mid-log phase was determined to be 3 h for *E. coli* and 5 h for *B. subtilis* for the present experimental conditions. The symbols \* + correspond to statistically different results between the control and the different SWNT samples, respectively.

1 The Live/Dead assay was performed to determine the viability of the bacterial cells after 1 h of  
2 incubation with the nanomaterials. For these experiments, only the most toxic concentrations of PVK-  
3 SWNT (*i.e.* 1 mg/ml for *E. coli* and 0.01 mg/ml for *B. subtilis*) were selected for incubation (Figure 2).  
4  
5 Fluorescence microscopy was used to assess the loss of bacterial viability after incubation. Figure 2  
6  
7 shows representative fluorescence images for the bacterial solutions incubated with the nanocomposite  
8  
9 PVK-SWNT and the control. Results show that in the absence of the nanomaterials, all cells were alive  
10  
11 (Figure 2a). While, cellular damage was observed in ~94 % and ~98 % of the *E. coli* cells exposed to  
12  
13 PVK-SWNT and SWNT, respectively. For *B. subtilis*, ~90 % and ~87 % of the cells were damaged after  
14  
15 exposure to PVK-SWNT and SWNT, respectively. The two most hypothesized mechanism of SWNT  
16  
17 toxicity to bacteria are physical disruption of bacterial membrane and oxidative stress.<sup>5, 7, 34-36</sup> From this  
18  
19 study, we can say that the addition of PVK did not prevent one of these two mechanisms to happen since  
20  
21 most of the cells exposed of PVK-SWNT were red-stained cells, which indicated that the PI dye could  
22  
23 penetrate inside the damaged cells.  
24  
25  
26  
27  
28  
29  
30  
31  
32  
33  
34  
35  
36  
37  
38  
39  
40  
41  
42  
43  
44  
45  
46  
47  
48  
49  
50  
51  
52  
53  
54  
55  
56  
57  
58  
59  
60

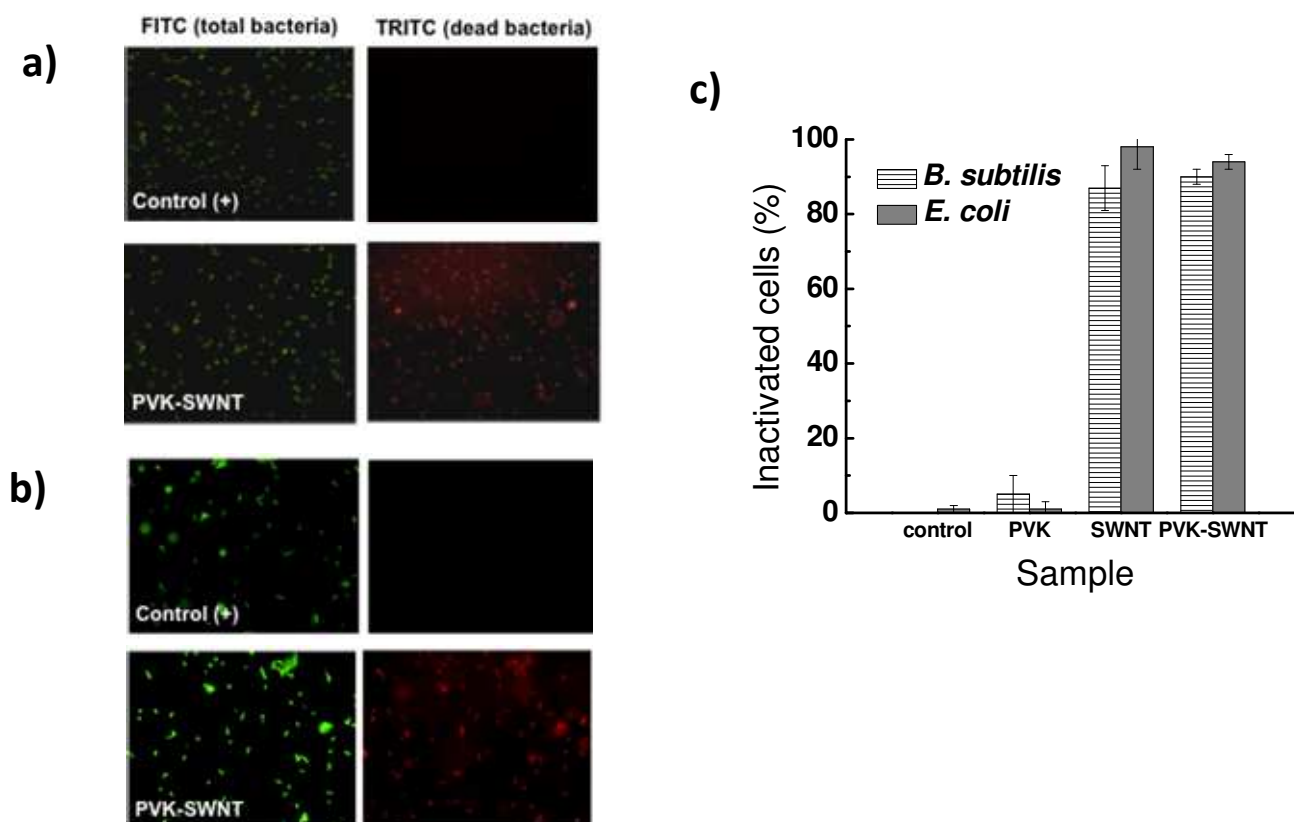


**Figure 2.** Viability assay for the bacteria exposed to nanocomposite: (a) Representative digital images after live and dead cell staining of *E. coli* exposed to PVK-SWNT and *E. coli* without the nanomaterial (control). (b) Representative digital images after live and dead cell staining of *B. subtilis* exposed to PVK-SWNT and *B. subtilis* without the nanomaterial (control). (c) Correlation of the % of non-viable *E. coli* and *B. subtilis* (Inactivated cells %) after exposure to PVK-SWNT, SWNT, and PVK.

*Biofilm growth inhibition in the presence of nanocomposites:* Although short term toxicity of SWNT on microbes has been extensively investigated by many researchers, there are only a handful of studies on long term toxicity effects of SWNT and SWNT nanocomposites on biofilm formation. In this study, we investigated toxic effects of PVK-SWNT and SWNT on biofilm formation for both *B. subtilis* and *E.*

*coli* through the crystal violet methodology.<sup>23</sup> The results showed (Figure 3) that less biofilm was formed after 48h exposure of *E. coli* and *B. subtilis* to PVK-SWNT and SWNT than the control. For *E. coli*, PVK-SWNT samples showed inhibition of biofilm growth by as much as ~13 % relative to the control; while for the SWNT samples, only ~5 % inhibition was observed. Similarly, for *B. subtilis*, both PVK-SWNT and SWNT samples showed the least biofilm growth, ~ 28%, relative to the control (Figure 3). In this study, it was demonstrated that in all SWNT and PVK-SWNT concentrations tested, significant biofilm formation inhibition happened to both *E. coli* and *B. subtilis*. This could be attributed to the better dispersion properties of PVK-SWNT samples. A similar study on inhibition of *E. coli* biofilm formation with pure SWNTs determined that the minimum concentration required for biofilm inhibition was 0.3 mg/ml, which was significantly higher than the concentration of SWNT used in our PVK-SWNT nanocomposite samples.<sup>7</sup> In general, for highly dispersed SWNT in nanocomposite samples, the results suggest that for long-term bacterial incubation and biofilm formation, higher SWNT concentrations (i. e. SWNT nanofiller concentration) have a greater inhibition effect. This inhibition can be achieved with increased SWNT concentrations because the ratio of SWNT to bacteria is probably high enough to inactivate most of the cells initially inoculated in the media, hence preventing cell recovery and biofilm formation.<sup>7</sup> The bacterial toxicity observed for the nanocomposite samples suggests that even for long-term bacterial exposure, the nanocomposite remained effectively toxic.



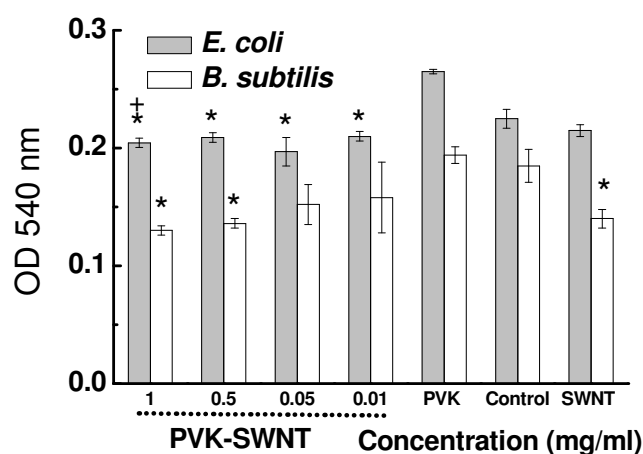


**Figure 3.** OD measurements obtained after biofilm test for the bacteria exposed to PVK-SWNT (97:3 wt % PVK:SWNT) at different concentrations. The symbols \* + correspond to result statistically different from the control and SWNT samples, respectively.

*Antimicrobial effects of PVK-SWNT nanocomposite immobilized on surfaces:* To demonstrate the efficiency of PVK-SWNT and SWNT as potential coating materials to prevent bacterial deposition and biofilm formation, the agar printing assay was performed with *E. coli* and *B. subtilis*. For this measurement, electrodeposited PVK-SWNT and spin-coated SWNT onto ITO surfaces were used. The nanocomposite-modified film contained 3 % SWNT and 97 % PVK. The results of PVK-SWNT were compared against electro-crosslinked PVK, spin-coated SWNT on ITO surfaces, and unmodified ITO surfaces as a control. The results showed that the percent bacterial inactivation on the coated PVK-SWNT surfaces compared to the unmodified ITO surfaces were 67% and 80 % for *B. subtilis* and *E. coli*, respectively (Figure 4). The PVK-coated surfaces did not show any antimicrobial property for neither *E. coli* nor *B. subtilis*, which suggests that the toxicity observed with the PVK-SWNT nanocomposite was due to the presence of SWNT only. Furthermore, these results show that antimicrobial activity for PVK-SWNT nanocomposite solutions were maintained even after electrodeposition.

Even though antibacterial properties of SWNT-coated surfaces were described in other studies, these studies used either pure SWNT or other nanocomposite materials than PVK for short incubation time.<sup>7, 34, 36</sup> However, this study is the first one to demonstrate that very low concentrations of SWNTs can be embedded in nanocomposites without losing its antimicrobial properties after prolonged exposure to bacteria (i. e. 48 h). In this study we embedded only 3% of SWNT in PVK-SWNT, which achieved almost similar inhibitory effects as 100 % SWNT (Figure 4). Furthermore, this study shows that the use of PVK improves dispersibility of SWNT in aqueous solution, achieving a more homogenous deposition of SWNTs onto surfaces<sup>22</sup> and at the same time maintaining the antimicrobial property of SWNT.

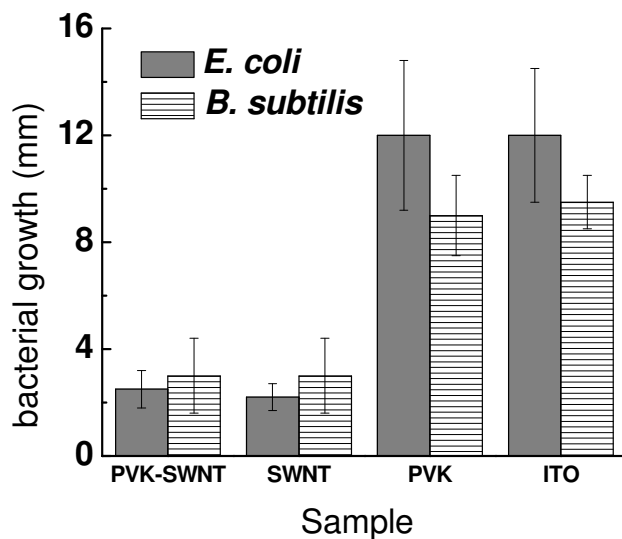


**Figure 4.** Agar printing assay to determine the survival of bacteria deposited onto ITO surfaces containing electrodeposited PVK-SWNT (97:3 wt% PVK:SWNT), spin coated SWNT (1 mg/ml), and electrodeposited PVK. Bare ITO surfaces were used as control. The amount of growth around the ITO coated and non-coated surfaces were determined using a caliper micrometer.

To investigate the long-term bacterial toxicity of the electropolymerized PVK-SWNT films, biofilms were allowed to grow for 48 h on modified ITO surfaces. The biofilm growth and area covered by microbial growth on the surface were determined by AFM. As control, AFM images of the electropolymerized PVK, spin-coated SWNT, and the unmodified ITO substrate were also taken. The results show that biofilms were able to grow on unmodified ITO and PVK films after prolonged exposure to *E. coli* (Figure 5) and *B. subtilis* (Figure S5). However, on electrodeposited PVK-SWNT

and SWNT films, just a few cells, but not a biofilm, were observed on the surface after 48 h exposure. These observations demonstrate that the nanocomposite-modified surface can effectively prevent biofilm growth the same way as pure SWNT films.<sup>7</sup> LIVE/DEAD staining and imaging of the bottom layer of the biofilm in direct contact with SWNT and PVK-SWNT surfaces showed that ~80 to 90% of the cells were dead for both *E. coli* and *B. subtilis*. Whereas only ~ 3 to 10% bacterial cells were dead on bare ITO surfaces (Figure S6). These results are in agreement with previous studies where small amounts of incorporated SWNT into polylactic-co-glycolic acid (PLGA) or polysulfonate (PSF) exhibited almost equivalent toxicity of 100 wt% SWNT coated surfaces.<sup>7, 36</sup> The mechanism of SWNT nanocomposites on bacterial colonization inhibition have been suggested as the direct contact of bacteria with SWNT ends and bundles that extend from the nanocomposite.<sup>36</sup> It is possible that our system (PVK-SWNT films) follows similar toxicity mechanism. It is worth noting that the PVK-SWNT nanocomposite can be electrodeposited onto any conducting surface, which in terms of cost and ease of application is significantly better than 100% SWNT coatings.

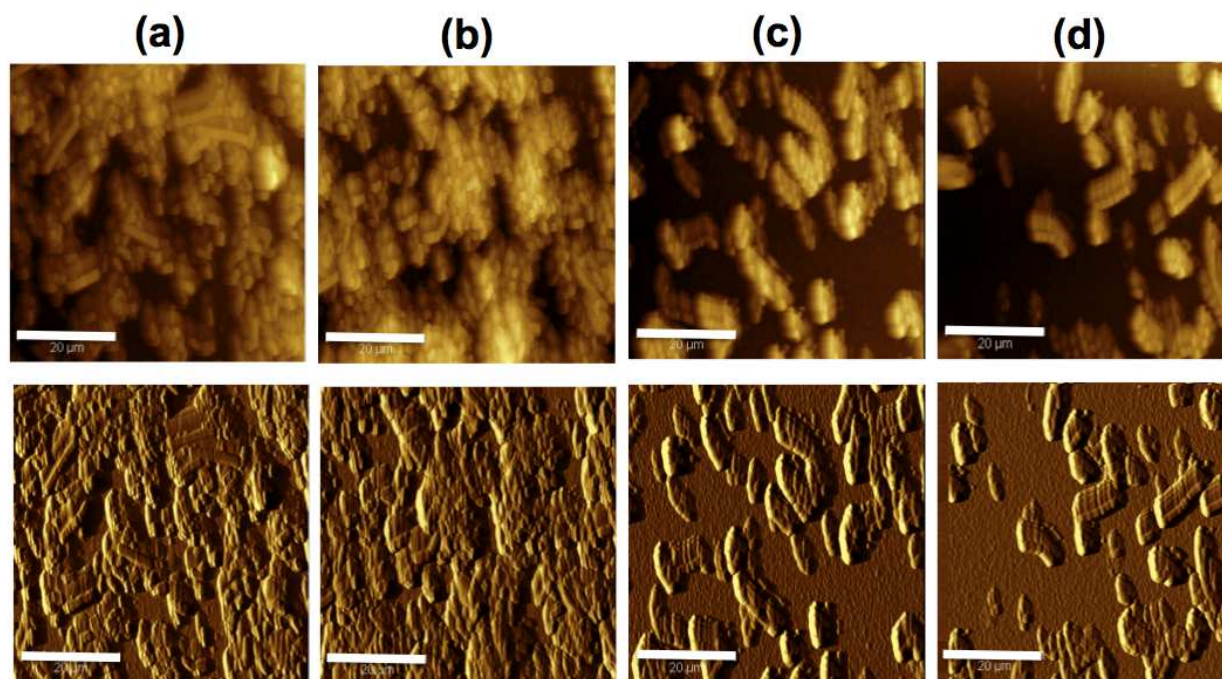


**Figure 5.** AFM (top) topography and (bottom) amplitude images of biofilm formation of *E. coli* on (a) ITO, (b) electrodeposited PVK (c) SWNT, and (d) PVK-SWNT coated surfaces. (Scale: 20  $\mu$ m)

1 Overall, this study shows that SWNT can be embedded into the electroactive polymer PVK to form  
2 stable PVK-SWNT nanocomposite dispersions and films. This mixture increased the dispersion and  
3 effective bacterial toxicity of SWNT into aqueous media and led to a more homogeneous coating of  
4 PVK-SWNT on ITO surfaces via electrodeposition. In both suspension and coated form, PVK-SWNT  
5 exhibited stronger antibacterial effects to *E. coli* and *B. subtilis* when compared to SWNT and PVK  
6 alone. Increasing loads of SWNT in the PVK-SWNT nanocomposite showed higher toxic effects to  
7 bacteria in both planktonic and biofilm phases. PVK-SWNT, with only 3% SWNT (0.03 mg/ml of  
8 SWNT), exhibited similar or stronger antibacterial effects than 100% SWNT (1 mg/ml of SWNT). Our  
9 study demonstrated for the first time that by improving dispersibility of SWNT in solution, higher  
10 bacterial toxicity of SWNT can be achieved. These results also demonstrated that it is possible to obtain  
11 more economical SWNT antimicrobial coated surfaces by significantly reducing the need of higher  
12 loads of SWNT when embedding the SWNTs in the polymer PVK.  
13  
14  
15  
16  
17  
18  
19  
20  
21  
22  
23  
24  
25  
26  
27

28 **Acknowledgement:**

29  
30  
31 The authors would like to acknowledge University of Houston New Faculty Research Program, proposal  
32 # 102556.  
33  
34  
35  
36

37 **Supporting Information:**

38  
39 Supplementary data associated with this manuscript is provided in the Supporting Information section.  
40  
41  
42  
43  
44  
45  
46  
47  
48  
49  
50  
51  
52  
53  
54  
55  
56  
57  
58  
59  
60

## References

1. Venkata, K. K. U.; Venkataramana, G., Appreciating the role of carbon nanotube composites in preventing biofouling and promoting biofilms on material surfaces in environmental engineering: A review. *Biotechnol. Adv* **2010**, 28, 802-816.
2. Morikawa, M., Beneficial biofilm formation by industrial bacteria *Bacillus subtilis* and related species. *J. Biosci. Bioeng* **2006**, 101, 1-8.
3. Münstedt, H.; Kumar, C. R., Silver ion release antimicrobial polyamide/silver composites. *Biomaterials* **2005**, 26, 2081-2088.
4. Radheshkumar, C.; Munstedt, H., Antimicrobial polymers from polypropylene/silver composites-Ag release measurement by anode stripping voltammetry. *React Funct Polym* **2006**, 66, 780-788.
5. Aslan, S.; Codruta, Z. L.; Kang, S.; Elimelech, M.; Pfefferle, L. D.; Paul, R. V. T., Antimicrobial biomaterials based on carbon nanotubes dispersed in poly(lactic-co-glycolic acid). *Nanoscale* **2010**, 2, 1789-1794.
6. Palmer, R. J.; White, D. C., Developmental biology of biofilms: implications for treatment and control. *Trends. Microbiol* **1997**, 5, 435-440.
7. Rodrigues, D.; Elimelech, M., Toxic Effects of Single-Walled Carbon Nanotubes in the Development of *E. coli* Biofilm. *Environ. Sci. Technol* **2010**, 44, 4583-4589.
8. Akasaka, T.; Watari, F., Capture of bacteria by flexible carbon nanotubes. *Acta. Biomater* **2009**, 5, 607-612.
9. Kang, S.; Mauter, S. M.; Elimelech, M., Physiochemical determinants of multiwalled carbon nanotube bacterial cytotoxicity. *Environ. Sci. Technol* **2008b**, 42, 7528-7534.
10. Narayan, R. J.; Berry, C. J.; Brigmon, R. L., Structural and biological properties of carbon nanotube composite films. *Mater. Sci. Eng* **2005**, 123 B, 123-129.

11. Nepal, D.; Balasubramanian, S.; Simonian, A. L.; Davis, V. A., Strong antimicrobial coatings: single walled carbon nanotubes armored with biopolymers. *Nano. Lett* **2008**, *8*(7), 1896–1902.
12. Zhu, Y.; Ran, T.; Li, Y.; Guo, J.; Li, W., Dependence of cytotoxicity of multi walled carbon nanotubes on the culture medium. *Nanotechnology* **2006**, *17*, 4668–4674.
13. Arias, L. R.; Yang, L., Inactivation of bacterial pathogens by carbon nanotubes in suspensions. *Langmuir* **2009**, *25*, 3003–3012.
14. Venkata, K. K. U.; Shuguang, D.; Martha, C. M.; Geoffrey, B. S., Application of carbon nanotube technology for removal of contaminants in drinking water: A review. *Science of the Total Environmt* **2009**, *408*, 1–13.
15. Q, L.; Mahendra, S.; Lyon, D. Y.; Brunet, L.; Liga, M. V.; Li, D.; Alvarez, P. J. J., Antimicrobial nanomaterials for water disinfection and microbial control: Potential applications and implications. *water. Research* **2008**, *42*, 4591–4602.
16. Cui, K. M.; Tria, M. C.; Pernites, R. B.; Binag, C. A.; Advincula, R. C., *ACS Applied Materials & Interfaces* **2011**.
17. Yeh, J. M.; Chang, K. C., *J. Ind. Eng. Chem* **2008**, *14*, 275.
18. Guimarda, N. K.; Gomez, N.; Schmidt, C. E., Conducting polymers in biomedical engineering. *Prog. Polym. Sci* **2007**, *32*, 876–921.
19. Santos, C. M.; Tria, M. C.; Vergara, R. A. M. V.; Ahmed, F. A.; Advincula, R. C.; Rodrigues, D., Antimicrobial graphene polymer (PVK-GO) nanocomposite films. *Chem. Commun.* DOI: [10.1039/c1cc11877c](https://doi.org/10.1039/c1cc11877c).
20. Ahujaa, T.; Ahmad, I.; Kumara, M. D., Biomolecular immobilization on conducting polymers for biosensing applications. *Biomaterials* **2007**, *28*, 791–805.
21. Frackowiak, E. b.; Beguin, F., Interaction between electroconducting polymers and C60. *Journal of Physics and Chemistry of Solids* **1996**, *57*, 983–989.

22. Cui, K. M.; Tria, M. C.; Pernites, R. B.; Binag, C. A.; Advincula, R. C., Carbon Nanotube-PVK Electropolymerized Conjugated Polymer Network Nanocomposite Films. *ACS Applied Materials & Interfaces* **2011**.
23. Pratt, L.; Kolter, R., Genetic analysis of Escheria coli biofilm formation: roles of flagella, motility, chemotaxis and type 1 pili. *Mol. Microb* **1998**, *30*, , 285-293.
24. Yang, C.; Mamouni, J.; Tang, Y.; Yang, L., Antimicrobial Activity of Single-Walled Carbon Nanotubes: Length Effect. *Langmuir Article* **2010**, *26*, 16013-16019.
25. Fox, E. N.; Demaree, R. S. J., Quick bacterial fixation technique for scanning electron microscopy. *Microscopy Research and Technique* **1999**, *46*, 338-339.
26. Fulghum, T. M.; Taranekar, P.; Advincula, R. C., Grafting Hole-Transport Precursor Polymer Brushes on ITO Electrodes: Surface-Initiated Polymerization and Conjugated Polymer Network Formation of PVK. *Macromolecules (Washington, DC, U. S.)* **2008**, *41*, (15), 5681-5687.
27. Ambrose, J. F.; Nelson, R. F., Anodic Oxidation Pathways of Carbazoles. *Journal of Electrochemical Society* **1968**, *115*, (11), 1159-1164.
28. Baba, A.; Onishi, K.; Knoll, W.; Advincula, R. C., Investigating Work Function Tunable Hole-Injection/Transport Layers of Electrodeposited Polycarbazole Network Thin Films. *J. Phys. Chem. B* **2004**, *108*, (49), 18949-18955.
29. Lyon, D.; Fortner, J. D.; Sayes, C. M.; Colvin, V. L.; Hughes, J. B., Bacterial cell association and antimicrobial activity of a C-60 water suspension. *Environ. Toxicol. Chem* **2005**, *24*, 2757–2762.
30. Lyon, D. Y.; Alvarez, P. J. J., Fullerene Water Suspension (nC60) Exerts Antibacterial Effects via ROS-Independent Protein Oxidation. *Environ. Sci. Technol.* **2008**, *42*, (21), 8127-8132.
31. Kang, S.; Mauter, M. S.; Elimelech, M., Microbial Cytotoxicity of Carbon-Based Nanomaterials: Implications for River Water and Wastewater Effluent. *Environmental Science & Technology* **2009**, *43*, (7), 2648-2653.
32. Kang, S.; Mauter, M. S.; Elimelech, M., Microbial cytotoxicity of carbon based nanomaterials: Implication of river water and wastewater effluent. *Environ. Sci. Technol* **2009**, *43*, 2648-2653.

1  
2  
3  
4  
5  
6  
7  
8  
9  
10  
11  
12  
13  
14  
15  
16  
17  
18  
19  
20  
21  
22  
23  
24  
25  
26  
27  
28  
29  
30  
31  
32  
33  
34  
35  
36  
37  
38  
39  
40  
41  
42  
43  
44  
45  
46  
47  
48  
49  
50  
51  
52  
53  
54  
55  
56  
57  
58  
59  
60

33. Mohanty, B.; Verma, A. K.; Claesson, P.; Bohidar, H. B., Physical and anti-microbial charecteristics of carbon nanoparticles prepared from lamp soot. *Nanotechnology* **2007**, *18*, 1-9.

34. Kang, S.; Herzberg, M.; Rodrigues, D. F.; Elimelech, M., Antibacterial Effects of Carbon Nanotubes: Size Does Matter! *Langmuir* **2008**, *24*, (13), 6409-6413.

35. Kang, S.; Pinault, M.; Pfefferle, L. D.; Elimelech, M., Single-walled carbon nanotubes exhibit strong antimicrobial activity. *Langmuir* **2007**, *23*, (17), 8670-8673.

36. Schiffman, J. D.; Elimelech, M., Antibacterial Activity of Electrospun Polymer Mats with Incorporated Narrow Diameter Single-Walled Carbon Nanotubes. *Acs Applied Materials & Interfaces* **2011**, *3*, (2), 462-468.